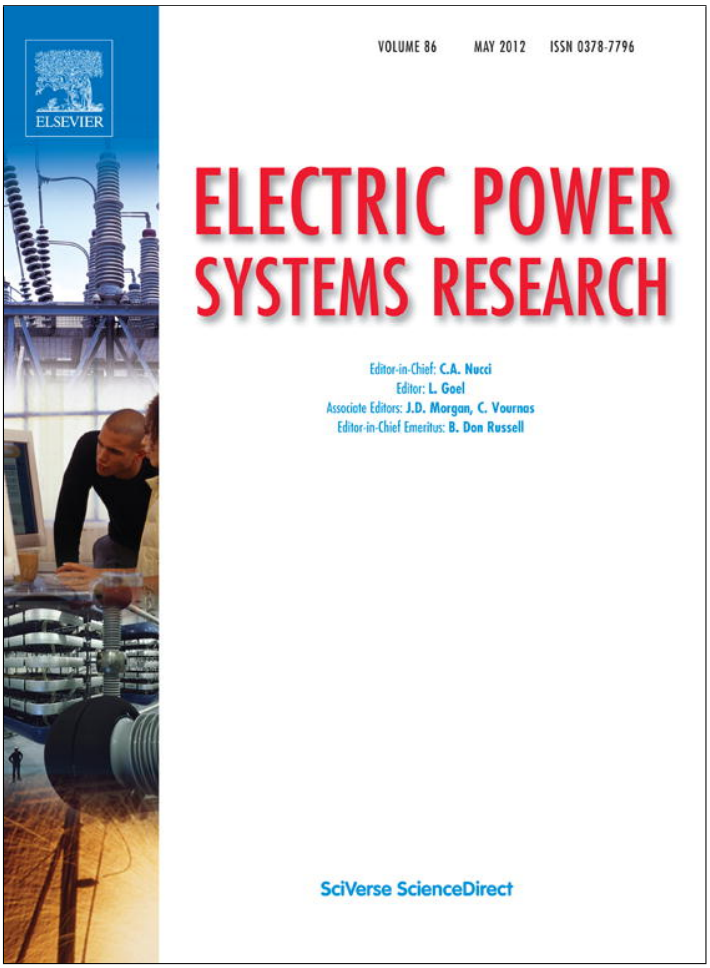

Electric Power Systems Research 86 (2012) 41–50

Contents lists available at SciVerse ScienceDirect

Electric Power Systems Research

journal homepage: www.elsevier.com/locate/epsr

Optimal sizing and operation of pumping systems to achieve energy efficiency and load shifting

He Zhang, Xiaohua Xia, Jiangfeng Zhang*

Department of Electrical, Electronic and Computer Engineering, University of Pretoria, Pretoria 0002, South Africa

ARTICLE INFO

Article history:
Received 27 April 2011
Received in revised form
26 September 2011
Accepted 1 December 2011
Available online 28 December 2011

Keywords:
Pumping system
POET framework
Energy efficiency
Load management
Capacity selection
Optimal control

ABSTRACT

Energy efficiency improvement for pumping system is an important problem for industrial energy systems. This article aims to improve pump efficiency by an approach based on energy efficiency classifications. To this purpose, an optimal pump sizing model is presented for new pumping system design, and an optimal pump operational control model is also given for existing pumping systems to minimize energy consumption cost and improve energy efficiency. Closed-loop model predictive control strategy is further applied for the pump operational control. These models show that the energy efficiency classification in terms of system performance, operation, equipment and technology (POET) is applicable to the pumping system energy efficiency study. Examples are given to illustrate the proposed models, which also convince the applicability of POET energy efficiency classification in the pumping system study.

1. Introduction

About 20% of all industrial electricity is consumed worldwide by pumping systems alone [1]. The dominant type of pump by far is the centrifugal pump, and it can easily become a source of poor efficiency unless properly designed, installed, and operated. It is a common practice for companies, even nations, to setup a power consumption reduction target for their pumping systems. For these reasons, the centrifugal pumping system is an ideal and meaningful subject for efficiency improvement through methods such as demand side management (DSM).

DSM was first introduced during the 1970s energy crises with the aim to deliberately influence customer appliance selections and energy usage patterns to achieve a desired impact or load shape [2]. According to [3] DSM can be divided into two categories, energy efficiency (EE) and load management (LM). Some articles prefer to exclude EE from DSM and form a separate EE category such as [4]. Despite different definitions of DSM, definitions of EE and LM are fairly consistent. EE aims to reduce the net amount of energy consumed, whilst LM aims to reduce the load in the peak demand period. The most common form of LM method is load shifting (LS). For LS, the operations are shifted as much as possible from periods of high energy demand to low energy demand [3].

Time-of-use (TOU) tariff is often used by utilities to encourage the implementation of LS. TOU tariff is based on higher rate during high demand periods and lower rate for the low demand periods. Some utilities also apply maximum demand (MD) tariff, which is an additional fee that must be paid based on the maximum power consumption. To facilitate the discussion, this article considers the case that the utility has both the TOU and MD tariffs.

Today, DSM is gradually transforming from a command and control with incentives stage, where DSM is driven by the utility or the state in the form of direct command or incentives, into a customer driven and customer finance stage [5]. In the current competitive business environment, only DSM that makes "good financial sense" will be pursued [5]. Hence the aim of DSM has shifted more and more toward operational energy cost reduction.

In [6] different system efficiency components are summarized into four categories, namely performance, operation, equipment and technology (POET). Performance efficiency of an energy system is determined by external but deterministic system indicators such as production, cost, energy sources, environmental impact, technical indicators and others. Operational efficiency is evaluated by the proper physical, time and human coordination of different system components. Equipment efficiency is a measurement of the energy output of isolated individual energy equipment with respect to the given technology design specifications. Technology efficiency is decided by the efficiency of energy conversion, processing,

* Corresponding author. Tel.: +27 12 420 4335; fax: +27 12 362 5000.
E-mail addresses: hzhang@tuks.co.za (H. Zhang), xxia@postino.up.ac.za (X. Xia), zhang@up.ac.za (J. Zhang).

0378-7796/$ – see front matter © 2011 Elsevier B.V. All rights reserved.
doi:10.1016/j.epsr.2011.12.002

transmission and usage. Technology efficiency is often evaluated by feasibility, life-cycle cost and return on investment [7]. Note that operation efficiency is sub-divided into three components, namely, physical, time and human coordinations [7]. In a water pumping system, physical coordination is the matching and sizing of different system components such as pump capacity, water flow rate, water heads, etc.; time coordination is the real time power consumption control to match the TOU tariff and water demand; and human coordination is the influence of human skills and experiences. Note further that pumping system load shifting is indeed a strategy to take advantage of the energy storage facility, the reservoir, so that more energy is consumed at cheap tariff period while less energy is consumed at expensive tariff period. Therefore, load shifting under a TOU tariff is a typical example for the time coordination control where water flow rate and the on/off status of the pump are controlled to meet the water demand and at the same time to minimize the energy cost. Hence, the energy efficiency of a pumping system can be greatly improved by studying its operation efficiency.

In this article, a pump operation efficiency improvement strategy is proposed based on the operation category of the POET framework. The operational efficiency is measured in monetary values, in other words the actual operational energy cost. The proposed pump operation efficiency improvement strategy focuses on the equipment-related physical and time coordinations of the operation category. Human coordination is not covered in this article. Nevertheless, human coordination is still a vital part of overall system operation, since humans are involved in every stage of the operation. Proper human coordination is essential for a pump system to operate at its optimal efficiency.

The main content of this article is divided into two parts in accordance to the physical and time coordinations categories. Their objectives are the optimal selection of the pump capacity based on operational EE and LS requirements and the design and test of a flexible pump closed-loop model predictive control (MPC) strategy that is capable of adapting to different system changes.

The term "flow rate" is used in this article to represent the actual output flow rate of a pump in m^3/h. The flow rate of a pump can be adjusted using devices such as valve or variable speed drive (VSD) controls. The term "system" of a pump refers to the piping network between the outlet of the pump and the pumping destination which is often a reservoir. The term "capacity" refers to the maximum operation output flow rate of a pump or a cluster of pumps. Capacity is different from the manufacturer specified maximum pump output flow rate, since the performance of a pump varies significantly with different system characteristics.

In this article, the optimal pump selection and control models are formulated for a multi-level pumping system. An example of a multi-level pumping system is shown in Fig. 1. The classification of the different levels is based on the pump arrangement. At each level there is one cluster of pumps. This cluster of pump can consist of one or more interconnected pumps that shares the same input and output pipes. However, it is possible to have multiple reservoirs at each level.

All of the optimization simulations are done on a mixed integer particle swam optimization platform.

2. Physical coordination

An important step toward an efficient system, according to the POET framework, is the matching of equipment to its operation requirements. There are a large number of existing pump selection algorithms available. In [8], the fundamental of EE based pump selection is illustrated. It is shown in this article that the energy cost is by far the biggest component in the pump life cycle cost. This article demonstrates that by carefully selecting the right pump the life cycle cost can be significantly reduced. Ref. [9] describes a method of determining the pump efficiency by conducting physical

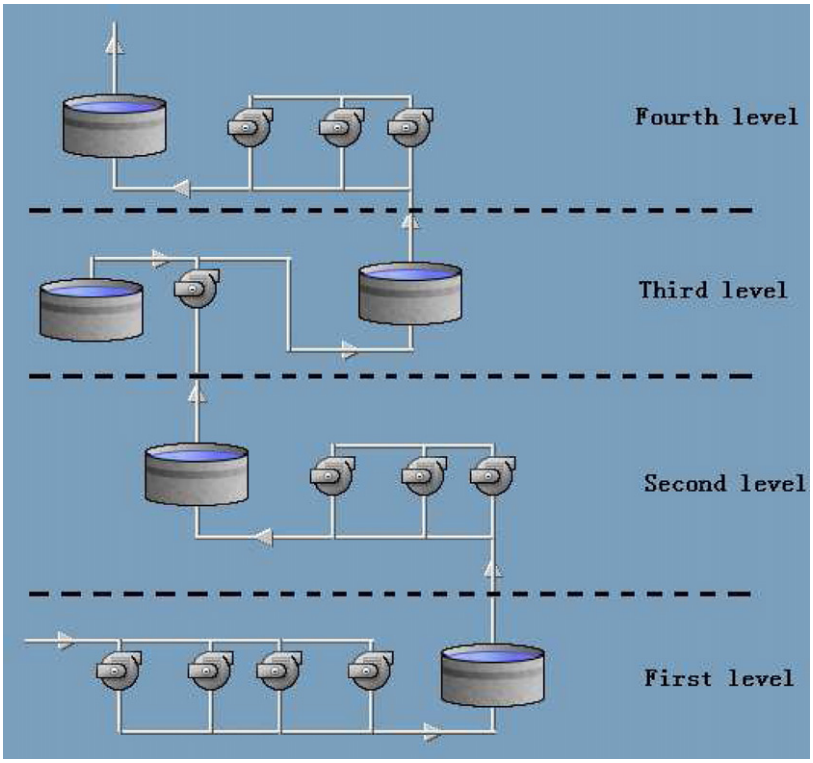

Fig. 1. Example of a multi-level pumping system.

measurements on the system before the actual implementation of the efficiency improvements. In [10], an optimization algorithm is used to select the best pump combination that will yield the highest operational efficiency based on how well the pumps characteristics match the system characteristics. In [11] an algorithm is derived to compute the ideal pump characteristics based on the system characteristics that will yield a minimal operational energy consumption. These existing pump selection studies in [8–11] focus on the maximization of pump EE by minimizing the total energy consumption. The selected pumping capacity is therefore minimal and additional capacity will be a waste of energy. In the case where a sufficiently sized reservoir is available as a buffer, the designer has more freedom to design the pumping capacity so that the energy cost can be minimized under a TOU tariff with load shifting techniques. This idea is formulated as an optimal pump capacity selection model in the following subsection.

2.1. Optimal pump capacity selection model

This section illustrates the formulation and verification of a optimal pump capacity selection model. The objective of this model is to optimally select the pumping capacity at each level of a multi-leveled pumping system by balancing LS and EE requirements.

The optimal pump selection in this article focuses only on the fixed speed pumps, since an optimally selected pump should not require additional investments on flow rate adjustment devices such as valves and VSDs.

The objective function of the optimal pump capacity selection model is given below,

$$\min_{u_{r,i},q_r} \sum_{r=1}^{R_c} \sum_{i=1}^{I_c} c_i f_r(q_r) u_{r,i} Z + M_{md} C_{md}, \tag{1}$$

where $f_r(q_r)$ is a function that computes the required input power for a given capacity at the r-th level. Also note that the product of I_c and Z represents the total number of control intervals in the control horizon.

For a multi-level pumping system, the optimal design problem is solved level-wise as shown in (1). q_r is the total pump capacity at the r-th and it is up to the designer to decide whether this capacity will be achieved using a single pump or a combination of multiple pumps. The operation of the pumps at the same level is controlled based on the computed optimal operational schedule represented by $u_{r,i}$. $u_{r,i}$ is restricted by the water level constraints of the reservoirs that have direct connections to the pumps.

The water levels of the reservoirs must not exceed their upper and lower limits at any time during the operation. Hence the optimization algorithm is bounded by the following constraint,

$$LL_j \le l_{j,i} \le UL_j : j = 1, \ldots, J_c. \tag{2}$$

The water level in the reservoir at the beginning of $(i+1)$-th operational interval can be defined as:

$$l_{j,i+1} = l_{j,i} + \sum_{r}^{R_c} a_{r,i} u_{r,i} - d_{j,i}. \tag{3}$$

This optimization model is formulated based on the tariff described in [12]. The MD tariff described in [12] is a monthly charge based on the recorded MD for that month. Hence the duration of the control horizon, which is represented by the product of I_c and Z should be equivalent in time to one month. For example, in a month of 30 days in which operation is assumed to repeat every 24 h, the choice of I_c and Z will be 24 and 30 respectively.

The MD is measured as the highest averaged demand in kVA during any complete half hour integrating period. The average power over a half hour interval (T, T+0.5) can be computed as,

$$2\int_{T}^{T+0.5} w(t)dt. \tag{4}$$

It is assumed that the operation of the pump and therefore the pump power consumption, $w(t)$, will be taken as a constant unit within a control interval. Therefore, by choosing a control interval duration that is greater than or equal to half an hour, the half hour MD period will fall completely within the control interval with the highest power consumption. The MD value will be approximately proportional to the power consumption of the control interval with the highest power consumption. Therefore, the MD value can be derived by,

$$M_{md} = \max\left\{ \sum_{r=1}^{R_c} f_r(p_r) u_{r,i} : i = 1, \ldots, I_c \right\}, \tag{5}$$

where max is a function that finds the maximum value within an array of data and $f_r(p_r)u_{r,i}$ is the power consumption of the r-th level at the i-th control interval.

The duration of the control interval is chosen to be one hour throughout this article. Other reasons for this choice are that the TOU tariff varies on an hourly basis and a longer duration reduces the wear and tear from regular operational adjustments.

The power consumption of a fixed speed pump can be assumed to be at a consistent level when the pump is active. Hence the MD value for a fixed speed pump can be assumed to be equal to the pump power consumption. The MD cost in (1) is computed based on the above assumptions and (5).

As shown in Refs. [13,14], the input power of a fixed speed pump can be computed using the hydraulic equation shown below with the power factor assumed to be 1,

$$p = \frac{9.81hq}{3.6\eta}. \tag{6}$$

The influence of the system on the performance of a pump can be described using a system curve. A system curve represents the relationship between water pressure or head (h) and the flow rate (q). This is a fixed and unique relationship for a given system and it represents the required pressure from the pump to achieve a particular flow rate within the system. This pressure is required to lift the water to the destination and overcome the friction of the pipes between the pump and its destination. This relationship is fixed regardless of the choice of pump. This relationship represented by the system curve can be estimated by the second order quadratic equation in (7).

$$h = Aq^2 + Bq + C. \tag{7}$$

The values of the constants A, B and C are unique and dependant on the shape of the system curve. These constants can be determined using methods such as interpolation.

In a multi-level pumping system, the piping arrangement at each level is different. Hence for every level of pumps, there is a unique system curve.

Substituting (7) into (6) yields an equation that relates the pump capacity to the pump input power. Take note that this capacity–power function is a third order function.

A pump capacity selection simulation is conducted under South African high demand season TOU tariff that is shown in Section 3.1 Fig. 5, sub-plot (a). In this simulation, a case study of one pump and one reservoir is considered such that the capacity selection ability of the algorithm can be focused on. The MD tariff is ignored for the purpose of a more clear demonstration of a balanced EE and LS pump capacity selection. I_c is 24 h. The pump is pumping into the reservoir; $d_{j,i}$ is chosen to be constant at 70 m^3/h for all i and it is

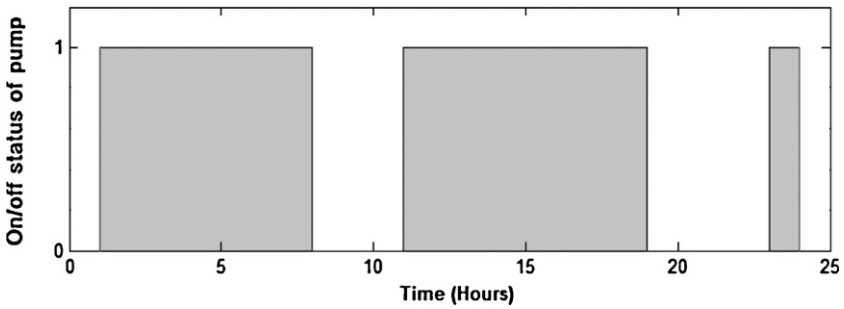

Fig. 2. Optimal schedule of the pump.

draining from the reservoir; the lower limit of the reservoir is set to be 500 m^3 and the upper limit is set to be at 1000 m^3.

The optimal pump capacity is computed as 103.023 m^3/h. The corresponding optimal operation schedule and the reservoir level change are shown in Figs. 2 and 3 respectively.

Fig. 2 demonstrates that the pump has enough capacity to shift the entire load out of the peak period. In Fig. 3 it can be seen that during the 23-rd hour, which is the end of the peak period, the reservoir level is at the minimum level. These two figures demonstrate that the pump capacity is just enough to shift the load completely out of the peak period.

As seen in sub-plot (a) of Fig. 5, the peak energy price is about six times more expensive than the off-peak one, the LS component is expected to be the dominating saving contributor, and the algorithm to maximize the level of LS. The EE component only prevents the pump capacity from being greater than what is required from LS.

To prove that this solution is optimal, a series of simulations are conducted to investigate the changes in the energy cost associated with pump capacity selection. These simulations compute the operational energy costs for different pump capacities ranging from 70 m^3/h to 140 m^3/h. The operational parameters are the same as the previous optimal selection simulation. The simulated energy costs of the optimal operations of the different pump capacities are plotted in Fig. 4.

The typical pump capacity choice of an EE only optimal design algorithm is most likely to be just above 70 m^3/h and as seen from Fig. 4 the corresponding energy cost is very high. As pump capacity increases, more loads can be shifted out of the peak hours and the energy cost is reduced. The optimal pump capacity shown is 103 m^3/h. At this point the pump manages to shift all of the loads out of the peak period. Additional increase in pump capacity offers no additional LS savings. As mentioned earlier, the capacity–power function is a cubic one and a small increase in the capacity results in much greater input power and energy consumption increase. Therefore beyond the optimal point further capacity increase only results in an increase in the energy cost.

It can be seen that LS and EE are two contradictory terms, the improvement of the one is at the cost of sacrificing the other. The optimal capacity selection model maximizes the saving contributions of LS and EE to minimize the operation energy cost.

Additional simulation is conducted under the high demand TOU tariff with a reservoir size that is insufficient to support a high level of LS. The upper limit of the reservoir is set to be 700 m^3 while the lower limit remains at 500 m^3. The computed optimal pump capacity is 90.588 m^3/h. This is significantly lower than the previous case. Since the level of LS is restricted by the reservoir size, there is no need for such a high capacity pump. Hence the algorithm chooses the smallest pump capacity that is capable of achieving the limited level of LS.

2.2. Optimal design limitations

Rigidness is an issue of optimal design. The optimal design tends to lose its optimality when the operational parameters change, for example change in tariff and demand. Designers often have to compensate for the risks of parameter variation by designing for the worst case scenario, which will significantly reduce operational efficiency.

Ideally, a flexible pump control mechanism can be used to compensate for this design rigidness. This flexible controller should be easily adjusted to adapt to the system changes without additional hardware modifications, ensuring that the operational energy cost remains minimal.

3. Time coordination

The time coordination section of the operation category focuses on the optimal control of the pump operation. In the early days of pump utilization, valves were used to control the output rate of the pump. Valve control is still widely used today, because it has the advantages of being cheap and simple to implement. However, pumps controlled by valves have very poor EE [15].

In recent years, VSD has been utilized to replace valve control to improve the pump EE. Refs. [15,16] are the illustrations of the

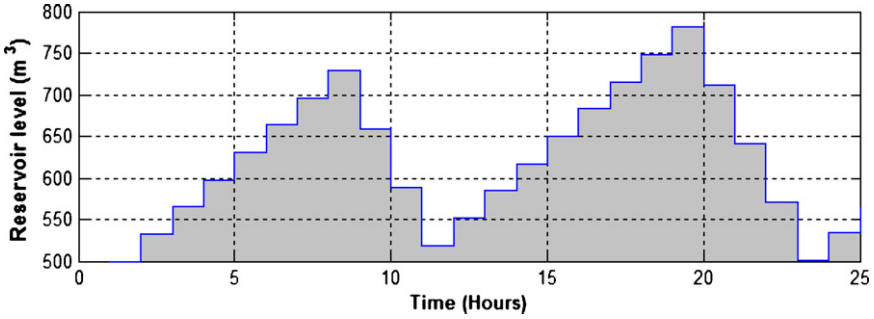

Fig. 3. Change in reservoir level.

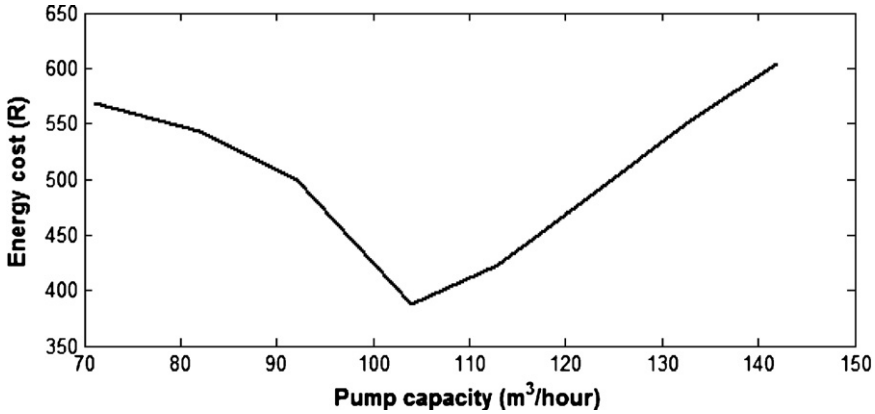

Fig. 4. Relationship of operational energy cost and pump capacity.

implementations and benefits of VSD in actual industrial applications. Refs. [17,18] are of more advanced control methods in which the input power is minimized by implementing model based optimization to control VSD driven pumps. All of the above articles are EE based.

LS is also widely implemented in pumping operations. Refs. [19–22] are examples of pump LS. These articles cover most LS scenarios such as, single pump operation [19]; multiple pumps operation [20]; operating under both TOU tariff and MD tariff [21]; and optimizing multiple objectives [22]. In all of the above cases an optimization model is used to compute a set of operation schedules based on the physical constraints and different tariff structures; all the pumps are controlled with on-off controllers; and a reservoir is in place for operation schedule changeability.

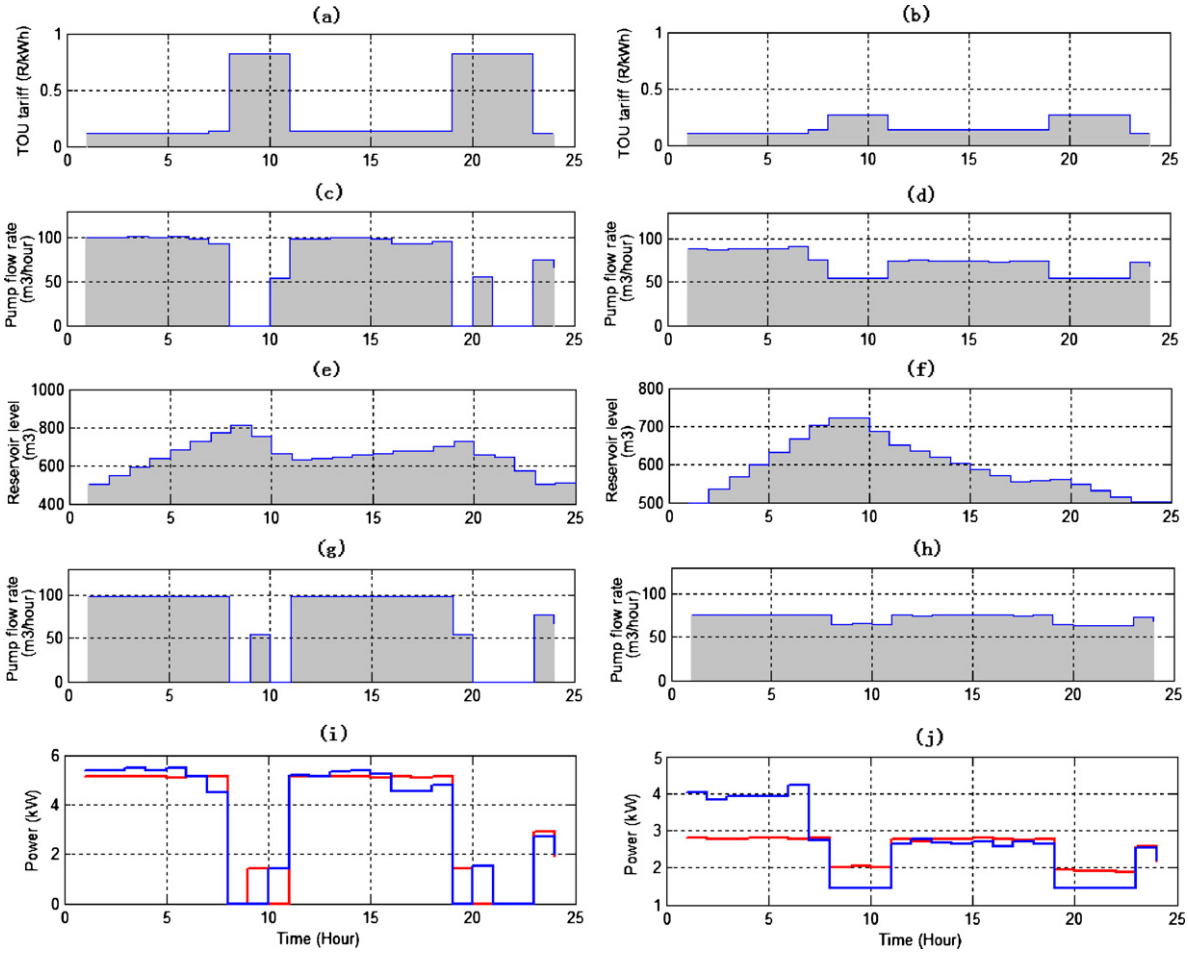

Fig. 5. Graphical summary of the VSD on/off controller simulation, (a) high demand TOU tariff; (b) low demand TOU tariff; (c) operation under high demand TOU; (d) operation under low demand TOU; (e) reservoir level change corresponding to (c); (f) reservoir level change corresponding to (d); (g) operation under high demand TOU and MD; (h) operation under low demand TOU and MD; (i) power consumption comparison of (c) and (g); (j) power consumption comparison of (d) and (h). (For interpretation of the references to color in the text, the reader is referred to the web version of this article.)

The only studies found to implement both EE and LS in one pumping project are [23,24]. However, [23] is not a true EE improvement since the overall efficiency is boosted by using the pump as a turbine to generate electricity when it is profitable to do so. Ref. [24] was initially an LS project but after implementation it was found that the overall efficiency was improved by chance.

Ref. [25] successfully implemented both EE and LS in a single belt conveyor system utilizing a VSD. This article demonstrates the flexibility of the VSD based controller, which is ideal for the compensation of the design rigidness. Since both belt conveyor and pump are motor-driven devices with similar properties, VSD should also be used to formulate an EE and LS combined pump control for a pumping system.

Closed-loop control, such as the MPC, has shown its ability to correct system and operation deviations and allows automatic control in studies such as [19,25]. Implementing closed-loop control is one of the best ways to increase the robustness of the control system under uncertainties. In this article, a closed-loop MPC approach is implemented.

The rest of this section is divided into two parts. The first part illustrates the formulation and testing of the open-loop pump optimal control strategy that combines EE and LS in the optimal control of the pump operation. The second part is the formulation and testing of the MPC. This proposed pump optimal control strategy is referred to as the VSD on/off controller.

3.1. Open-loop VSD on/off controller

As the name implies, this system consists of both a VSD and an on/off controller. The reason for an on/off controller operating together with the VSD controller is that a centrifugal pump can only operate above a given minimum motor rotation speed, otherwise the water will just swirl within the tubes and nothing will be pumped out [26]. Unlike in the case of conveyor belt [25], the speed of the VSD can be adjusted from 0 to maximum without any problem. Operating a pump below its minimum motor rotation speed will not only waste energy but also cause the pump to overheat. The VSD therefore only has a small range of speed adjustment typically between 25% and 50% of the maximum motor rotation speed. This limited range of adjustment significantly restricts the level of LS and the associated savings for VSD controlled pumps.

To solve this problem, the controller must switch off the pump completely when the operation is below the minimum motor rotation speed. Hence an on/off controller is used together with the VSD controller. Normally the on/off controller is on and the VSD is responsible for all the flow rate adjustments. When the ideal motor operating speed is below the minimum speed, the on/off controller will take over, switch the pump off and achieve the necessary LS.

The VSD on/off control is best suited for single pump operations, in other words, one pump at each level. The purpose of the VSD is to allow flow rate adjustments. For multiple interconnected pumps in a same level, the adjustment in the net flow rate can be achieved by switching on different number of pumps. This type of multi-pump control is an effective energy cost reduction strategy as shown in [20]. Utilizing VSD on/off control in multiple interconnected pumps operational control will offer more precise control and further improved in EE, however, these improvement might not be significant enough to justify the initial cost, since the VSD on/off control requires a VSD for each pump. Therefore, for multiple interconnected pumps operation the method illustrated in [20] is recommended. For the rest of the text, it is assumed that there is only one pump at each level of the multi-level pumping system.

The objective of the optimal control is to minimize energy cost of a multi-level pumping system over a control horizon. The energy cost consists of TOU and MD tariff. The objective function is defined in (8).

$$\min_{q_{r,i},u_{r,i}} \sum_{r=1}^{R_c}\sum_{i=1}^{I_c} v_r(q_{r,i})u_{r,i}c_i Z + C_{md}M_{md}, \tag{8}$$

where $v_r(q_{r,i})$ is the flow–power function that computes different input power in kW corresponding to different flow rate of a variable speed pump at the r-th level; and N_{md} is the function that finds the MD value within a control horizon and it is formulated based on (5) shown in (9).

$$M_{md} = \max\left\{\sum_{r=1}^{R_c} v_r(p_{r,i})u_{r,i} \ : i = 1,\ldots,I_c\right\}. \tag{9}$$

The more advanced VSDs are capable of power factor corrections [27], hence the power factor can be assumed to be 1.

The optimal values of variables $q_{r,i}$ and $u_{r,i}$ need to be solved by the optimization algorithm over the control horizon.

The water level constraint described by Eq. (3) also applies to this optimal control model.

The capacity–power function of (6) provides a crude estimation of the relationship between the pump capacity and the input power. This capacity–power function is sufficient for the process of fixed speed pump capacity selection. However, this is insufficient for the variable speed pump optimal control application. A more complex flow–power function that includes the effects of motor rotational speed changes on the flow rate and input power, must be derived.

This flow–power function is derived from [28], where the input power of a pump at different operating speed is mathematically computed using the pump characteristic information, pump motor rotational speed and system characteristics.

The pump characteristic information is summarized in the pump performance curves and power curves found in the manufacturer's data booklet. The pump performance curves represent the relationship between the operational flow rate, q, and the generated pressure, h, of the pump under different motor rotational speeds in rpm, n. The power curves indicate the required input power in kW, p, for different flow rates at different speeds.

The relationships represented by the pump performance curves and the power curves can be estimated by (10) and (11) respectively [28].

$$h = Dq^2 + Esq + Fs^2, \tag{10}$$

$$p = Gq^3 + Hq^2 s + Iqs^2 + Js^3. \tag{11}$$

Constants D to J are similar to A to C of (7) in the sense that they are also fixed and unique for a particular pump. These constants can also be obtained using interpolation method based on the pump characteristic curves. From the Nomenclature, the ratio s satisfies

$$s = \frac{n}{n_{full}}. \tag{12}$$

From (7) and (10) a function that defines the relationship between the motor rotation speed and the flow rate can be formulated and this relationship can be estimated using (13),

$$s = Kq + L, \tag{13}$$

(13) can be used to compute the VSD speed control settings based on the required flow rates.

The flow–power function can be derived from (13) and (11). The result function can be estimated using a third order polynomial shown in (14),

$$p = Mq^3 + Nq^2 + Oq + P. \tag{14}$$

This flow–power function is unique and fixed for a particular pumping system. The values of the constants K to P are dependant on the values of constants A to J.

The proposed optimal control algorithm is simulated based on a case study of one pump and one reservoir to illustrate the operation of the proposed control model. In this case study the controlled pump is pumping fresh water into the reservoir while the water demand is draining from the reservoir.

The hourly water demand (d_i) for 24 h is described in (15).

$$d_i = \left\{ \begin{array}{ll} 55, & i \in [0, 8] \\ 90, & i \in [8, 16] \\ 70, & i \in [16, 24] \end{array} \right\}. \quad (15)$$

The pump used for this case study is a K80-250 model from KSB, and its performance characteristics can be found in [29], motor rotation speed flow rate function for this case study is computed to be,

$$s = 0.0071q + 0.2791 \quad (16)$$

The maximum and minimum motor rotation speeds are 1450 and 960 rpm. The corresponding maximum and minimum flow rates are 102 m^3/h and 54 m^3/h respectively. The upper and lower limits of the reservoir are 1000 m^3 and 500 m^3. The flow–power function of the pump is formulated as,

$$p = (3.8969e - 6)q^3 + (2.1851e - 5)q^2 + 0.01117q + 0.13102. \quad (17)$$

Simulation are conducted under different tariff structures that include high and low demand TOU with or without MD tariff and the results are summarized in Fig. 5.

In Fig. 5 subplots (a) and (b) illustrate the 24 h electricity price variation for the high and low demand TOU tariff.

Subplot (c) illustrates the pump flow rates under high demand TOU tariff. Since the electricity price during peak hours is significantly higher, the algorithm shifts the loads as much as possible to the off-peak and standard periods. This is clearly illustrated during the morning peak hours (8:00–11:00) where the on/off controller switches off the pump completely. During the evening peak hours (19:00–23:00) the pump has to be switched on twice to prevent the reservoir level dropping below the lower limit. When the pump is switched on during the peak hours, it is operating at the minimum operational flow rate to keep the cost down.

Subplot (d) shows the pump flow rates under low demand TOU tariff. Sub-plot (d) differs significantly from sub-plot (c). The most significant difference is that the pump is no longer switched off during peak hours but rather operating at a lower rate. Since the peak-hour electricity price of the low demand TOU tariff is much lower than the high demand one, it becomes more profitable to sacrifice some of the LS for EE. As mentioned earlier, a slight reduction in the flow rate results in a significant reduction in power consumption. Therefore, by operating the pump during peak hours, the overall pump flow rate in other periods can be reduced. The overall EE is improved and energy consumption cost is reduced.

The corresponding reservoir level variations of the pump operation described in sub-plot (c) and (d) are shown in sub-plots (e) and (f). It can be seen that the reservoir level constraints are satisfied.

Sub-plot (g) shows the pump flow rates under high demand TOU with MD tariff. In sub-plot (g), the output flow rates of the pump are more even and leveled in the periods outside the peak hours in comparison to sub-plot (c). This is due to the effect of the additional MD tariff. As mentioned earlier, the MD tariff is a charge based on the maximum power demanding period. In order to minimize this cost, the algorithm spreads the loads out as evenly as possible and therefore limits the pump to operate at a slightly lower and constant rate. The maximum flow rate is reduced by 2.8% in sub-plot (g) in comparison to (c). Sub-plot (i) illustrates the differences in the power consumptions of the pump flow rate settings presented in sub-plot (c) and (g). The blue line represents the power consumption of sub-plot (c) and the red line represents sub-plot (c). Since the flow–power function is cubic, this maximum flow rate reduction of 2.8% is amplified to a 6.62% reduction in the MD.

The pump flow rates under summer TOU and MD tariff is shown in sub-plot (h). As expected, the flow rates are leveled at a very constant rate. The peak hour operation is further increased to allow a further reduction in the maximum flow rate and MD cost. The MD is reduced by 34.12% in sub-plot (h) in comparison to (d).

Sub-plot (j) illustrates the differences in power consumption of the flow rate settings presented in sub-plot (d) and (h). The MD is reduced by 34.12% in this case. The reason for such a high level of reduction in MD in comparison with the high demand TOU case is that the average energy cost of the low demand TOU tariff is much lower than the average energy of the high demand TOU tariff and the additional MD tariff has a much greater weight in the total operational cost in the low demand case. Hence greater effort is spent to reduce the MD cost.

Sub-plot (c) demonstrates the LS capability of the VSD on/off control; sub-plot (d) illustrates the ability of the VSD on/off control to freely adjust the contributions from EE and LS to minimize the energy cost; sub-plots (g) and (h) demonstrate that the VSD on/off control is also capable to minimize the MD and the associated charges.

In order to evaluate the financial benefit of the proposed VSD on/off control system, the operation energy cost of VSD on/off control is compared to the energy cost of four existing pump control methods. The four other pump control methods are, valve control, VSD control (EE only initiative), level based on/off control and optimal LS control. These four control methods are simulated alongside the proposed VSD on/off control with the same operation parameters under different tariff structures. The different tariff structures considered are, high demand TOU without/with MD tariff, low demand tariff without/with MD tariff and flat tariff without/with MD tariff. The simulated operation energy costs of the different control methods are summarized in Fig. 6. The blue columns represent the monthly energy costs the red columns represent the MD cost and the green columns represent the savings in comparison to the valve control.

As shown in Fig. 6, the valve control has the highest energy cost and the level based on/off control has the second highest. The energy cost of the VSD control and optimal LS control varies significantly with different tariff structures. These two controls alternate the third and fourth highest energy cost positions for different tariff structures. The proposed VSD on/off control achieves the lowest energy cost under all scenario considered. These results illustrate that the VSD on/off control is capable of adapting to different tariff and effectively reducing the operation energy cost.

3.2. Closed-loop MPC

The objective function in (8) is modified into an objective function and it is defined in (18),

$$\min_{q_{r,i}, u_{r,i}} \sum_{r=1}^{R_c} \sum_{i=1+m}^{I_c+m} v_r(q_{r,i}) u_{r,i} c_i Z + C_{md} M_{md}, \quad (18)$$

where $m = 1, \ldots, M_{mpc}$ and M_{mpc} represents the last switching interval. M_{mpc} can be considered as infinite if the controller is running none stop. The control horizon of (18) is over (m, $m + I_c$).

In (18) the open-loop optimal control problem is solved repeatedly over a finite control horizon at each control interval i, and only the first control step is implemented after each iteration. At the next control interval ($i + 1$) the reservoir level is sampled again and the

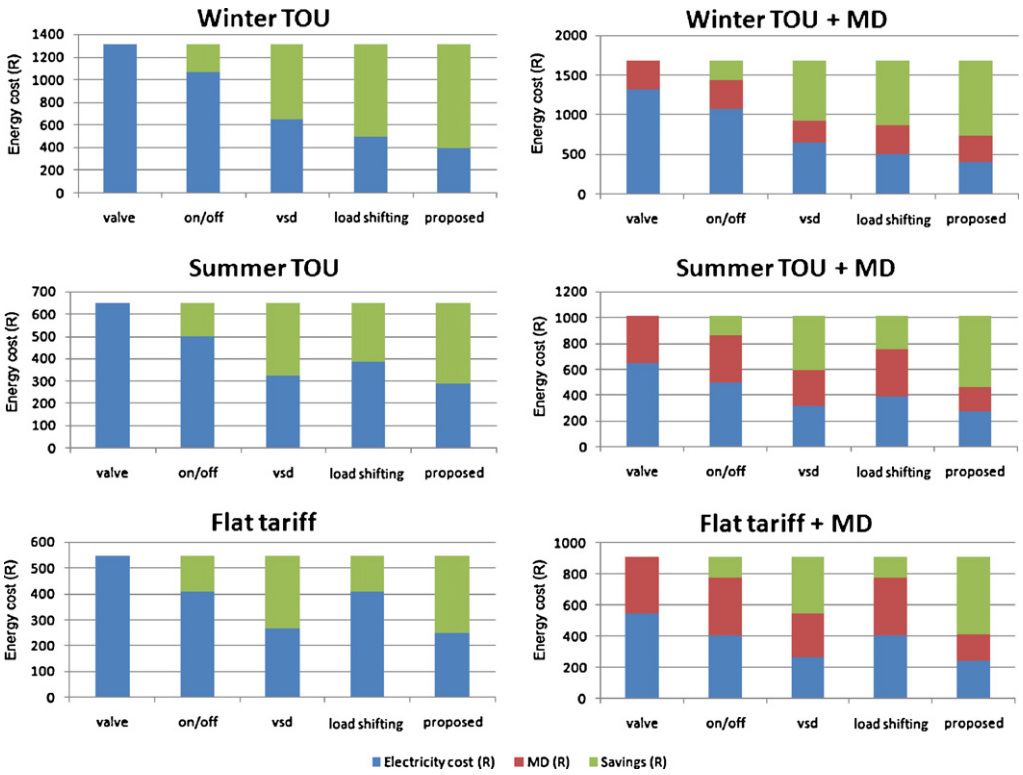

Fig. 6. Operational energy costs comparison of different control strategies under different tariff structures. (For interpretation of the references to color in the text, the reader is referred to the web version of this article.)

process of optimization is repeated over the new control horizon $[m, I+m]$.

The reservoir level constraint of the open-loop model also applies to the closed-loop model. The only difference is that this constraint needs to be updated after each control interval is implemented.

The greatest motivation for the implementation of the closed-loop MPC approach is the improvement it brings about in the system's robustness. The following simulation illustrates how the MPC control model detects and compensates for the errors in the system.

The control model is simulated for 48 h. The operational parameters are the same as in Section 3.1 for the first 24 h. At the beginning of the 25-th hour an additional constant 20 m^3/h water demand is introduced such that,

$$d_{i+24} = d_i + 20, : i = 1, 2, \ldots, 24. \tag{19}$$

This additional demand increase could be due to a leakage or additional water demand. The only communication between the control model and the actual plant is through the reservoir level feedback. The control model is unaware of the water demand increase and continues to use the forecasted water demand in (15) to compute the flow rate. The 48 h water demands profile, flow rate and the reservoir level variations are plotted in the demand, flow rate and reservoir level sub-plots of Fig. 7.

The process of detecting and correcting the error can be divided into two stages, which are indicated by the different color shades in Fig. 7.

The first stage, indicated by the yellow-shaded area, is when the error is not significant enough to be noticed by the control model, and there is no significant difference in the flow rates compared to the corresponding time slot of the previous 24 h. Although the reservoir level is lower than what it should have been because of the accumulation of the additional water demand, it is still significantly above the lower limit and does not cause much of a problem to the control model. It can be seen that the reservoir level is still sufficient to allow LS to take place in the 32-th hour.

At the 34-th hour, the pump has to be switched on to keep the water level above the limit. It means that the errors in the system have accumulated to an extent, such that drastic measures have to take place. This marks the start of the second stage, the active correction stage, indicated by the blue shaded area.

Since the peak time electricity price is very high under high demand TOU, it is mandatory to operate the pump at the minimum flow rate. The flow rates during the peak hours should only be sufficient to keep the water level just above the limit. Unfortunately this minimal flow rate is computed by the control model based on the forecast demand of water, and in this case the forecast demand is much lower than the actual one. This results in a much lower flow rate than what is actually required, which leads to the reservoir level dropping below the allowed limit during the 35-th hour.

At the beginning of the 36-th hour, a violation of the water level constraint is detected, and the highest priority of the control model is to increase the water level to above the minimum level as soon as possible. However, the water demand, from the 33-rd to the 41-st hour, are higher than the full capacity of the pump. Despite the efforts of the pump operating at full power and sacrificing the MD savings, the water level continues to drop until the high water demand period ends.

Hours 42–46 are evening peak hours. It can be seen that very little LS took place, and savings from LS are further sacrificed in an attempt by the control model to correct the water level. Very limited LS occurred only during the 45-th and 46-th hour.

Because of the efforts of the MPC control model, the water level is stabilized and is almost at the acceptable level by the end of the 48-th hour. Fig. 8 shows the same simulation but with the open-loop control model.

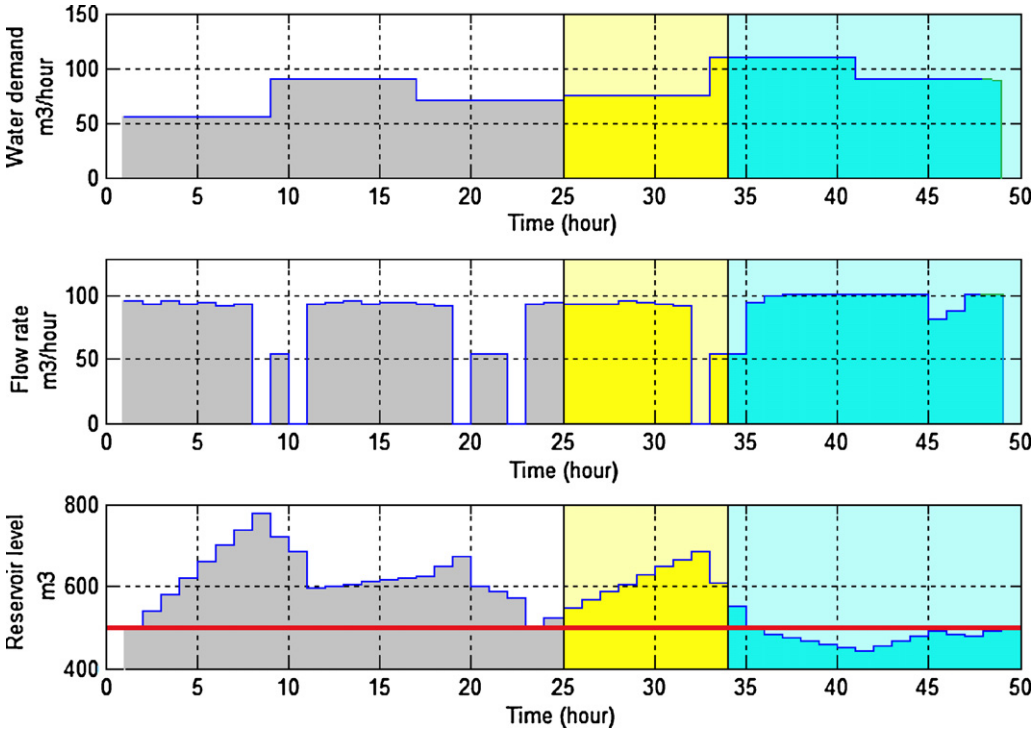

Fig. 7. Illustration of the MPC control strategy robustness. (For interpretation of the references to color in the text, the reader is referred to the web version of this article.)

In the case of the open-loop control model, there is no feedback; the model is isolated from the actual plant and unaware of any changes in the system. The error will continue to accumulate without any correction and eventually lead to a possible system failure. This is illustrated in Fig. 8, where the reservoir level has dropped to almost 0.

The 24-h water demand from the 25-th to 48-th hour is increased to 2200 m^3 from the 1720 m^3 level of the previous 24 h. The MPC control model pumped a total of 2151.73 m^3 of water from the 25-th to the 48-th hour while the open-loop model only pumped 1723.13 m^3. The volume of water pumped in the MPC case is very close to the actual demand, and significantly higher than

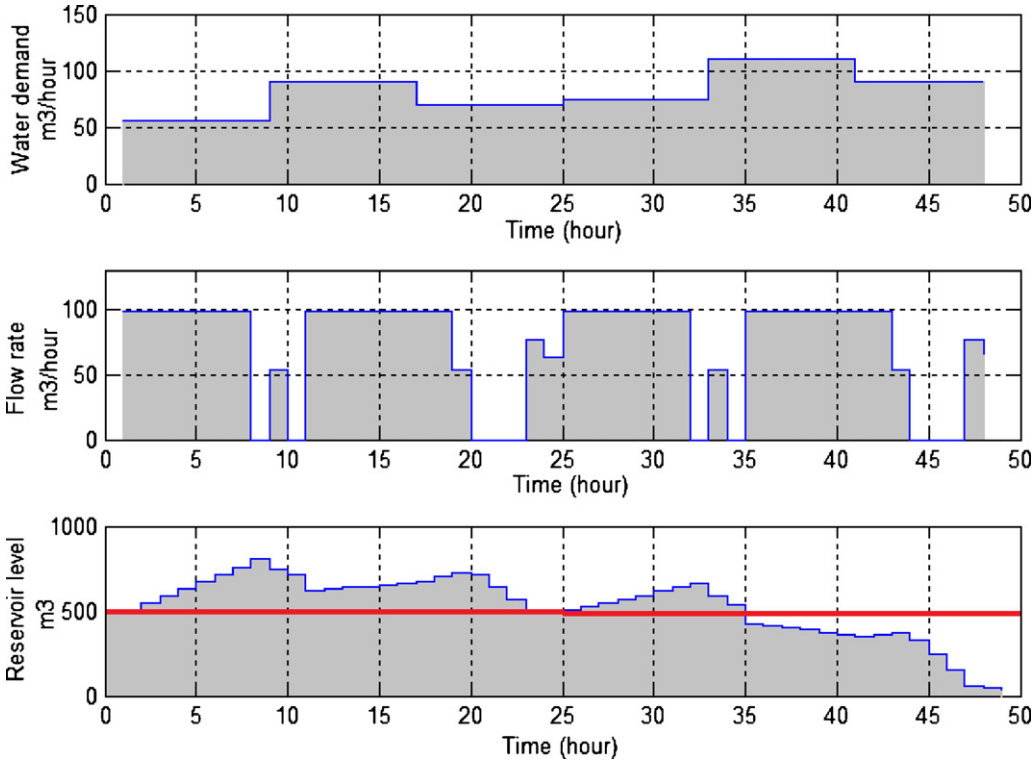

Fig. 8. Illustration of the open-loop optimal control model operation with demand variation.

that in the open-loop case. This further illustrates the benefit of the robustness of the MPC control model.

MPCs are also suitable for automatically resolving a host of other system errors, such as design mistakes and poor modeling accuracy. The mechanisms of error correction are the same as in the above simulation.

4. Conclusion

This article derives a water pumping operation energy cost reduction strategy based on the POET framework. This derivation affirms the validness and applicableness of the POET framework. An optimal pump capacity selection model is also proposed and verified. In this model, additional capacity requirements for load shifting are considered along with the traditional energy efficiency requirements. It is shown that if a facility is charged under a time-of-use tariff, it is more financially beneficial to include load shifting in the selection of the optimal pumping capacity. A pump optimal operation control strategy is proposed. This control strategy demonstrates the reduction in energy cost by balancing the energy efficiency and load shifting contributions during the operation. In addition, this control model is very flexible and can be adjusted to adapt to different operational conditions. Lastly, this article affirms the practical importance of model predictive control techniques.

Acknowledgment

The authors would like to thank the anonymous reviewers for the valuable comments.

Appendix A. List of symbols

r	index of pumping level, $r = 1, \ldots, R_c$
R_c	total number of pumping level
i	index of control interval, $i = 1, \ldots, I_c$
I_c	the number of control intervals in which all of the operation parameters can be assumed to be repeating
Z	the number of repeating cycles of duration I_c within the control horizon
$u_{r,i}$	the optimal on/off schedule of the pump at the r-th level
q_r	the capacity at the r-th level
c_i	the TOU energy cost for the i-th control interval in R/kWh
C_{md}	the MD tariff cost at 66.5 R/kVA
M_{md}	the function that finds the MD value within a control horizon
j	index of the reservoirs, $j = 1, \ldots, J_c$
J_c	the total number of reservoirs
LL_j	the lower level limits of the j-th reservoir
$a_{r,i}$	the flow rate of the r-th pump at the i-th control interval
UL_j	the upper level limits of the j-th reservoir
$d_{j,i}$	the net amount of water inflow or outflow of the j-th reservoir from sources other than the pumps in m^3/h
$w(t)$	the instantaneous power consumption in kW as a function of time t
T	the starting point of a half hour period
p	the computed input power to the pump in kW
q	the flow rate in m^3/h
h	the pump generated pressure in m
R	Rand, South African currency
$q_{r,i}$	the flow rate setting of the pump of the r-th level at i-th control interval
A, B, C	constants
s	the ratio between the actual motor rotation speed and the full motor rotation speed given in (12)
n	motor rotational speed
n_{full}	full motor rotational speed
η	the pump operational efficiency which is assumed to be a fixed value

References

[1] D. Hammerstorm, et al., Pacific Northwest GridWise test bed demonstration project. Part I: olympic peninsula project, Pacific Northwest Laboratory, PNNL 17167, 2007, pp. 5.1–5.6.
[2] J. Boivin, Demand side management—the role of the power utility, Pattern Recognit. 28 (1995) 1493–1497.
[3] D. Loughran, J. Kulick, Demand-side management and energy efficiency in the United States, Energy J. 25 (2004) 19–43.
[4] C. Gellings, The concept of demand-side management for electricity utilities, Proc. IEEE 73 (1985) 1468–1470.
[5] F. Sioshansi, Demand side management, the third wave, Energy Policy 23 (1995) 111–114.
[6] X. Xia, J. Zhang, Energy audit—from a POET perspective, in: Int. Conf. on Appl. Energy, Singapore, April 21–23, 2010, pp. 1200–1209.
[7] X. Xia, J. Zhang, Energy efficiency and control systems—from a POET perspective, in: IFAC Conf. on Control Methodologies and Technol. for Energy Efficiency, Vilamoura, Portugal, March 29–31, 2010.
[8] J. Tolvanen, Life cycle energy cost savings through careful system design and pump selection, World Pumps (July 2007) 34–37.
[9] M. Moreno, P. Carrion, Measurement and improvement of the energy efficiency at pumping stations, Biosyst. Eng. 98 (2007) 479–486.
[10] C. Pulido-Calvo, J. Gutierrez-Estrada, Optimal design of pumping stations of inland intensive fishfarms, Agric. Eng. 35 (2006) 283–291.
[11] M. Moreno, et al., Development of a new methodology to obtain the characteristic pump curves that minimize the total cost at pumping stations, Biosyst. Eng. 102 (2009) 95–105.
[12] Tshwane, Electricity tariffs for Tshwane metropolitan municipality. Available from: http://www.tshwane.gov.za.
[13] C. Vladimir, et al., Mathematical model for efficient water flow management, Nonlinear Anal. Real World Appl. 11 (2010) 1600–1612.
[14] M. Yin, J. Andrews, Optimum simulation and control of fixed-speed pumping stations, Environ. Eng. 122 (1996) 205–211.
[15] G. Irvine, I. Gibson, The use of variable frequency drives as a final control element in the petroleum industry, in: Ind. Appl. Conf. Rome, October 8–12, 2000, pp. 2749–2758.
[16] R. Errath, Ingrated variable speed drive—the energy saver, in: IEEE Cement Ind. Technical Conf., Mexico City, May 21–23, 1991, pp. 135–149.
[17] X. Meng, H. Wang, Application of hybrid genetic algorithm in frequency speed control pumping station, in: 4th Int. Conf. on Natural Computation, Shan Dong, China, June 12–14, 2008, pp. 337–341.
[18] Bortoni, et al., Optimization of parallel variable speed driven centrifugal pumps operation, Energy Efficiency 3 (2008) 167–173.
[19] A.J. van Staden, J. Zhang, X. Xia, A model predictive control strategy for load shifting in a water pumping scheme with maximum demand charges, Appl. Energy 88 (2011) 4785–4794.
[20] W. Jowitt, G. Germanopoulos, Optimal pump scheduling in water-supply networks, J. Water Resour. Plann. Manage. 118 (1992) 406–422.
[21] G. McCormick, R. Powell, Derivation of near optimal pump schedules for water distribution by simulated annealing, J. Oper. Res. Soc. 55 (2004) 728–736.
[22] M. Lopez-Ibanez, Multi-objective optimization of the pump scheduling problem using SPEA2, Evol. Comput. 1 (2005) 435–442.
[23] F. Vieira, H. Ramos, Hybrid solution and pump-storage optimization in water supply system, Energy Policy 36 (2008) 4142–4148.
[24] E. Kamdem, Measurement and verification on combined load management and energy efficiency project, 2010. Available from: http://www.eskom.co.za/content/CombinedLM_EE.pdf.
[25] S. Zhang, X. Xia, Optimal control of operation of belt conveyor system, Appl. Energy 87 (2010) 1929–1937.
[26] L.T.D. Sulzer Brothers, Sulzer Centrifugal Pump Handbook, Elsevier Science Publishers Ltd., New York, 1989.
[27] P. Pulkki, Not just speed control, in: Cement Ind. Technical Conf., Finland, April 25–30, 2004, pp. 169–184.
[28] R. Carlson, The correct method of calculating energy savings to justify adjustable-frequency drive on pumps, IEEE Trans. Ind. Appl. 36 (2000) 1725–1733.
[29] KSB, Volute Casing Pump Offer Curves, KSB Industry, 2007.